Electrolyte gate controlled metal-insulator transitions of the CaZrO3/SrTiO3 heterointerface

Niu, Wei; Chen, Yongda; Gan, Yulin; Zhang, Yu; Zhang, Xiaoqian; Yuan, Xiao; Cao, Zhi; Liu, Wenqing; Xu, Yongbing; Zhang, Rong

Total number of authors:
14

Published in:
Applied Physics Letters

Link to article, DOI:
10.1063/1.5108813

Publication date:
2019

Document Version
Publisher's PDF, also known as Version of record

Applied Physics Letters

Electrolyte gate controlled metal-insulator transitions of the $CaZrO_3/SrTiO_3$ heterointerface

Cite as: Appl. Phys. Lett. **115**, 061601 (2019); https://doi.org/10.1063/1.5108813
Submitted: 02 May 2019 . Accepted: 10 July 2019 . Published Online: 05 August 2019

Wei Niu, Yongda Chen, Yulin Gan, Yu Zhang, Xiaoqian Zhang, Xiao Yuan, Zhi Cao, Wenqing Liu, Yongbing Xu, Rong Zhang, Nini Pryds, Yunzhong Chen, Yong Pu, and Xuefeng Wang

Applied Physics Letters ARTICLE scitation.org/journal/apl

Electrolyte gate controlled metal-insulator transitions of the $CaZrO_3/SrTiO_3$ heterointerface

Cite as: Appl. Phys. Lett. **115**, 061601 (2019); doi: 10.1063/1.5108813
Submitted: 2 May 2019 · Accepted: 10 July 2019 ·
Published Online: 5 August 2019

View Online Export Citation CrossMark

Wei Niu,[1,2] Yongda Chen,[2] Yulin Gan,[3] Yu Zhang,[3] Xiaoqian Zhang,[2] Xiao Yuan,[2] Zhi Cao,[1] Wenqing Liu,[4] Yongbing Xu,[2] Rong Zhang,[2] Nini Pryds,[3] Yunzhong Chen,[3] Yong Pu,[1,a)] and Xuefeng Wang[2,a)]

AFFILIATIONS

[1]New Energy Technology Engineering Laboratory of Jiangsu Province & School of Science, Nanjing University of Posts and Telecommunications, Nanjing 210023, China
[2]National Laboratory of Solid State Microstructures, Collaborative Innovation Center of Advanced Microstructures and School of Electronic Science and Engineering, Nanjing University, Nanjing 210093, China
[3]Department of Energy Conversion and Storage, Technical University of Denmark, Risø Campus, Roskilde 4000, Denmark
[4]Department of Electronic Engineering, Royal Holloway, University of London, Egham, Surrey TW20 0EX, United Kingdom

[a)]**Authors to whom correspondence should be addressed:** puyong@njupt.edu.cn and xfwang@nju.edu.cn

ABSTRACT

Two-dimensional electron gas (2DEG) at a complex oxide interface shows an extraordinary spectrum of intriguing phenomena and functionality. Another oxide 2DEG was recently created via strain-induced polarization at an otherwise nonpolar perovskite-type interface of $CaZrO_3/SrTiO_3$ (CZO/STO). Herein, we report an effective way to tune the CZO/STO interface via ionic liquid (IL) electrolyte gating. An unexpected metal-insulator transition of the interfacial 2DEG occurs readily with the immersion of the sample in an IL even before the gate voltage is applied. This suggests the presence of intrinsic polarization of CZO, which could act as a negative bias. The carrier density is found to be suppressed and shows a temperature-independent behavior after electrolyte gating which also resulted in higher electron mobility. These results suggest that the oxygen vacancies are annihilated via oxygen electromigration to the interface induced by electrolyte gating. The effective tunability by IL gating shed more light on the mechanism of electrolyte gating on the buried heterointerface.

Two-dimensional electron gas (2DEG) at a complex oxide interface shows an extraordinary spectrum of emergent phenomena and functionality, spanning high electron mobility,[1] superconductivity,[2] magnetism,[3,4] quantum hall effect,[5] and giant tunability by multistimuli.[6–8] Among these intriguing properties, one defining characteristic is the critical thickness (t) for the occurrence of metallic interfaces. For example, when the thickness of the $LaAlO_3$ (LAO) capping layer is equal to or thicker than 4 unit cells (uc), an abrupt transition from an insulating to a conducting state occurs at the interface between LAO and $SrTiO_3$ (STO).[1,9] For a nonisostructural interface of γ-Al_2O_3/STO (GAO/STO), highly metallic 2DEG is generated when the t of GAO is above the threshold thickness of 2 uc.[10,11] Many possible mechanisms have been proposed to explain this striking generation of 2DEG,[12] such as electronic reconstruction due to polar discontinuity, La-doped STO via interfacial intermixing, and oxygen vacancies.[13] In particular, the explanation of polar discontinuity has drawn most attention due to the intrinsic doping of STO without disorder.[14] However, this mechanism only works under the condition where a polar overlayer, such as LAO, is grown on a nonpolar STO substrate.

Similar to polar discontinuity, 2DEG at the interface of AlGaN/GaN[15] and ZnO/ZnMgO[16] can also be generated due to spontaneous piezoelectric polarization. The top capping layer utilizes this polarization and drives electrons to the interface. Inspired by these observations of 2DEG in conventional semiconductors and a binary oxide heterointerface, Chen *et al.* have recently created a high mobility oxide 2DEG at an otherwise nonpolar isostructural perovskite-type interface of $CaZrO_3$/STO (CZO/STO) via strain-induced polarization.[14] It is found that a lattice displacement due to a compressive strain at the CZO film results in a polarization toward the interface.[14] This polarization drives the transfer of electrons from CZO to the STO, thus a 2DEG is formed at the interface. First-principles calculations have further confirmed this possibility of electron transfer at the interface of CZO/STO by strain-induced polarization.[17] Very recently, Levy *et al.* also demonstrated an extreme reconfigurable nanostructure with a featured size of 1.2 nm at the interface of CZO/STO using conducting Atomic Force Microscopy (c-AFM).[18]

To impart the desired intriguing properties of 2DEG, external stimuli are often used to control the behavior of the system. Nowadays, electrolyte gating with ionic liquids (ILs), utilizing an electronic double layer transistor (EDLT) configuration, has been developed as a powerful means.[19,20] The value of the carrier density can be modified as high as 10^{15} cm^{-2} with only a few volts, arising from the extremely large electric field formed at the nanogap electronic double layer.[19,20] With such a remarkable tunability, the resultant properties at interfaces can be manipulated. For example, the Kondo effect, ultrahigh mobility, and quantum oscillations in the LAO/STO system were induced via IL gating.[21,22] Our previous report also witnessed a giant tunability by IL gating, including the Kondo effect, tunable Rashba spin–orbit coupling, and Lifshitz transition of the 2DEG at the interface of GAO/STO.[23] Besides the electrostatic mechanism, an electrochemical effect based on ions moving in an IL could also control properties effectively.[24,25] Under such conditions, oxygen vacancies could be induced during the electrolyte gating process. An archetypal example is VO_2, where the formation of oxygen vacancies induced by IL gating suppresses its metal-insulator transition (MIT).[26] Beyond VO_2, many other systems, such as TiO_2,[27] STO,[28] $La_{0.8}Sr_{0.2}MnO_3$,[29] and $NdBa_2Cu_3O_{7-\delta}$,[30] also showed significant electrolyte gating induced oxygen vacancies. In contrast to the generation of oxygen vacancies, a recent report found that oxygen vacancies formed at the interface of LAO/STO (only amorphous LAO) could be annihilated during the electrolyte gating.[31] However, this remarkable electromigration capability to fill oxygen vacancies in the 2DEG at the interface between the single-crystal capping layer and STO has never been observed. Furthermore, so far, there is no report on the IL gating of 2DEG at a nonpolar perovskite-type interface, and the mechanism of electrolyte gating on the buried heterointerface remains elusive. Therefore, it is interesting to study with electrolyte gating the interface of CZO/STO.

Herein, we report an electrolyte gating on the 2DEG originating from the strain-induced polarization at the isostructural perovskite-type interface of CZO/STO. The corresponding carrier density (n_s) and mobility (μ) are effectively manipulated by IL gating utilizing the EDLT configuration. In particular, an unexpected MIT occurs at the interface with immersion in an IL even when no gate voltage is applied. This could be attributed to the strain-related intrinsic polarization of the CZO top overlayer. Besides the effective tunability of the conducting states at the interface of CZO/STO, our work also indicates the migration of oxygen (annihilation of oxygen vacancies rather than formation of oxygen vacancies) by electrolyte gating. In contrast to the degradation of samples during the electrolyte gating, the mobility of 2DEG at the CZO/STO interface is significantly improved via the migration of oxygen, i.e., less scattering sites for the electron.

CZO thin films were grown on TiO_2-terminated STO substrates, which were prepatterned in the Hall bar configuration by using amorphous $LaMnO_3$ as a hard mask, as schematically shown in Figs. 1(a) and 1(b). Details of the growth conditions and the fabrication process are described elsewhere.[11,14,23] The layer-by-layer growth mode was confirmed for the unpatterned samples, using *in situ* reflection high-energy electron diffraction (RHEED), as shown in Fig. S1 (supplementary material). The well-defined RHEED oscillation and RHEED patterns suggest the high quality of the as-grown CZO films. The epitaxial growth of the CZO film on the STO is further confirmed by AFM. As illustrated in Fig. 1(c), a terrace surface with a regular step height is clearly seen, further indicating the atomic smoothness of the as-grown sample.

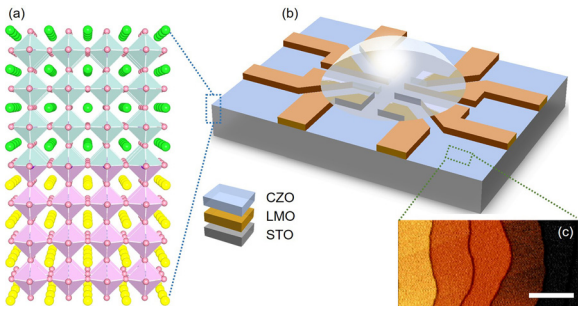

FIG. 1. (a) A sketch of the isostructural perovskite-type CZO/STO heterostructure. (b) The EDLT configuration for the CZO/STO Hall bar interface. (c) Surface AFM image of a 10-uc CZO film on STO. The scale bar is 500 nm.

For transport measurements, aluminum wire electrodes were bonded ultrasonically. The IL of 1-ethyl-3-methylimidazolium-bis(trifluoromethanesulfonyl)amide (EMI-TFSI) with poly-(styrene-block-methylmethacrylate-block-styrene) (PS-PMMA-PS) was chosen as the gate dielectric material due to its easy figurability[32] and high capacitance.[23] As displayed in Fig. 1(b), a small drop of the IL was placed on the surface. The IL can also be easily washed off using organic solvents, such as acetone and isopropanol. Note that devices with a typical CZO thickness of 10 uc were chosen to ensure both the metallic interface and the modest carrier density of $\sim 2 \times 10^{13}$ cm^{-2} at low temperatures. A Pt strip was used as the gate electrode without resistance hysteresis observed in the LAO/STO system previsouly.[33] Similar measurements were performed on several devices, all of them showing reproducibility and consistency.

Figure 2 shows the transport properties of a typical CZO/STO patterned heterointerface. The inset in Fig. 2(a) shows an optical micrograph of the Hall-bar heterointerfacial device. Temperature-dependent sheet resistance (R_s) is shown in Fig. 2(a); R_s drastically decreases with decreasing temperature (T) and saturates when the temperature is lower than 10 K indicating a typical metallic behavior,

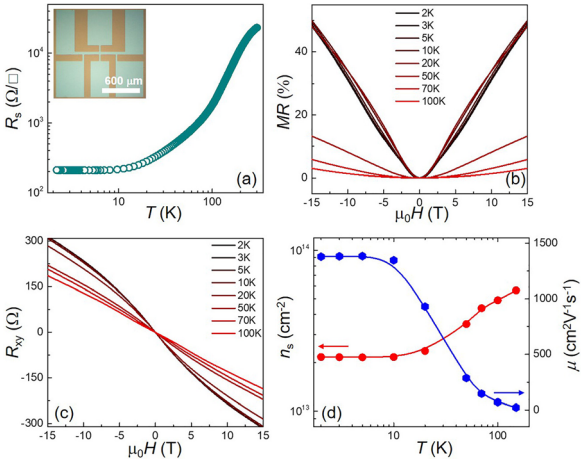

FIG. 2. Transport properties of a typical 10-uc CZO/STO heterointerface. (a) Temperature-dependent sheet resistance. Hall-bar configuration of the device is shown in the inset. (b) MR behavior of CZO/STO at different temperatures. (c) Hall resistance vs magnetic field at various temperatures. (d) Temperature dependence of carrier density, n_s, and mobility, μ.

in agreement with the previous reports.[14] Figure 2(b) shows magnetoresistance (MR) as a function of the applied magnetic field at different temperatures. Positive MR curves are observed over the whole temperature ranges, and the MR ratios [MR = $(R_{xx} - R_0)/R_0 \times 100\%$] are comparable to or even larger than those in previous 2DEG systems, such as LAO/STO and GAO/STO.[23,34] Figure 2(c) shows a magnetic field dependence of Hall resistance (R_{xy}). The n_s is derived from $n_s = -1/R_H \times e$ (R_H is the Hall coefficient) for linear R_{xy} when $T \geq 70$ K. Additionally, R_{xy} is found to be nonlinear when $T < 70$ K, indicating the presence of multiband transport carriers as observed in other 2DEG systems, such as LAO/STO[35–37] and GAO/STO.[23] A two-band model was fitted to deduce the n_s from the nonlinear R_{xy}.[23] The corresponding n_s and μ as a function of temperature are shown in Fig. 2(d). The carrier density decreases monotonously as the temperature decreases and then maintains an almost constant value of 2.17×10^{13} cm^{-2} at low temperatures. The carrier density exhibits a carrier freezing out behavior, which could be due to oxygen vacancies and the in-gap states, as commonly observed in the LAO/STO system.[31] The value of the mobility, on the other hand, decreases from ~1400 cm^2 V^{-1} s^{-1} at 2 K to 21 cm^2 V^{-1} s^{-1} at 150 K. Note that although the mobility at low temperature of the patterned device is not as high as one reported previously (for unpatterned samples measured in the van der Pauw configuration),[14] the measured μ in the current work is still relatively high compared with other 2DEG heterointerfaces that are patterned into Hall bar devices.[11,38]

The above measurements are performed on pristine samples without any IL or gating. A small drop of IL is then added that covered both the heterointerface with Hall-bar configuration and the Pt electrode to form the EDLT device under the gate voltages (V_g). When applying positive V_g, cations move close to the CZO/STO heterointerface, and correspondingly, anions move toward the gate electrode. (The essential concept of EDLT is illustrated in Fig. S2.) An electronic double layer with nanoscale thickness is therefore formed at the interface between the IL and the conducting channel. In contrast, cations and anions move toward the opposite direction, respectively, under the applied negative bias as compared with the positive gating process. The electronic double layer formed by the cations and carriers is essentially a nanogap supercapacitor, which has proved effective in tuning carrier densities and the electron migration.[19] Since the 2DEG in CZO/STO is of n-type, carriers could be accumulated (depleted) at the interface by applying positive (negative) V_g. Figure 3(a) shows the temperature-dependent R_s as a function of V_g. Performing a negative gate range of $V_g < 0$ V, R_s increases with decreasing temperature and becomes insulating well beyond the measurement limits when $T < 100$ K. This indicates the depletion of electrons by decreasing the electrostatic gate potential, which is consistent with the work mechanism of EDLT. Remarkably, a sharp MIT occurred at no gate voltage, $V_g = 0$ V, i.e., a metallic behavior is observed upon cooling at the range of $T > 40$ K, and then an abrupt MIT occurred at $T < 40$ K. Compared with the pristine metallic-conduction, it seems that the IL has a major influence on the performance of the interface even without gating. Notably, in the cases of crystalline samples of LAO/STO and GAO/STO, no obvious difference or such MIT was observed after immersing the interfaces in the IL (Fig. S3), thus we have excluded the contribution of polar adsorbates.[12,39] This giant change observed in the present study could be attributed to the presence of intrinsic polarization induced by strain at the interface of CZO and STO.[14,40] This phenomenon is also consistent with the fact that, before dropping the IL on the CZO surface, the R_s and n_s are ~1700 Ω/□ and 4.9×10^{13} cm^{-2}, respectively. However, R_s shifted to ~25 650 Ω/□ as well as the n_s is suppressed to ~5.5×10^{12} cm^{-2} after dropping the IL on the surface of the device (Fig. S4). This insulating tendency of the CZO/STO device at $V_g = 0$ V is in accordance with the results obtained by applying a negative V_g, i.e., increasing R_s and suppressing n_s.[23] By applying positive V_g, the device recovers the overall metallic behavior. With increasing V_g and subsequent electrostatic potential, the metallic state is significantly stabilized and improved owing to the accumulation of electrons at the interface.

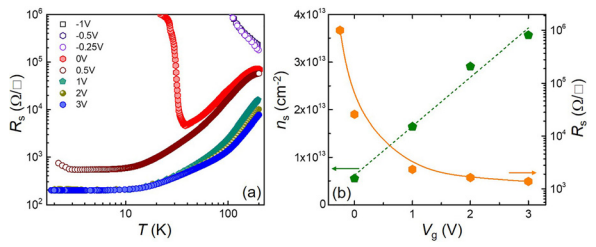

FIG. 3. MIT tuned by the IL gating. (a) Temperature-dependent sheet resistance under different gate voltages. (b) Underlying carrier density and mobility vs gate voltage at 100 K.

To fully demonstrate the modulation of sheet resistance and carrier density by IL gating, Fig. 3(b) quantitatively summarizes the tunability of R_s and n_s by electrolyte gating at 100 K: R_s decreases monotonously from around 1×10^6 Ω/□ to ~1370 Ω/□ as the voltage V_g increases from −0.25 V to 3 V. Moreover, n_s increases linearly from ~5.5×10^{12} cm^{-2} to ~3.6×10^{13} cm^{-2} over the positive gate range. The effective capacitance (C_g) of the electrolyte gating can be estimated from the linear V_g-dependent on n_s by using the formula $C_g = \frac{dn_s}{dV_g} \times e$.[21] Here, the C_g is estimated to be ~1.65 μF/cm^{-2}, which is slightly smaller than the one reported in a 3-uc LAO/STO heterointerface.[21] This relatively small capacitance could be ascribed to the fact that the conducting interface is buried under the 10-uc (~4 nm) CZO overlayer rather than on a bare channel surface[20] or a channel with a thinner capping layer.[21] The decreased R_s and the enhancement of n_s modulated by increasing the voltage, V_g, show the accumulation of electrons by the electrostatic gating as expected.

The ability to control the MIT, i.e., conductivity, is at the heart of modern electronics. We next explore whether the MIT at $V_g = 0$ V could be reversibly switched by immersion in the IL. After conducting the above gating experiments, the IL is rinsed by acetone and isopropanol and the device is then measured again. As displayed in Fig. 4(a), we compare the temperature-dependent R_s of the device before dropping the IL, with IL at $V_g = 0$ V and after removing the IL, respectively. Interestingly, the MIT vanishes and the interface recovers the metallic behavior over the full-temperature-range after washing off the IL. The conducting state of the interface improved, i.e., the higher R_s at the high temperature range, whereas the lower R_s at the low temperature region after removing the IL compared with the pristine ones, consistent with the system of amorphous LAO/STO heterointerface.[29] The corresponding n_s and μ before dropping and after removing the IL are shown in Fig. 4(b). For the pristine device before inserting the IL, the carrier density is kept constant at low temperatures, then increases upon increasing the temperature, this carrier freezing out behavior indicates the existence of oxygen vacancies. However, n_s is

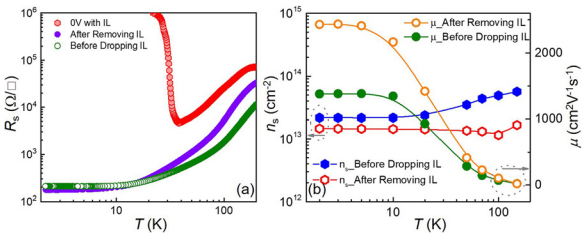

FIG. 4. Oxygen electromigration by electrolyte gating. (a) The temperature-dependent sheet resistance of the CZO/STO heterostructure before dropping the IL, with the IL, and after removing the IL, respectively. (b) The temperature dependence of carrier density and mobility before dropping the IL and after removing the IL.

kept nearly constant at $\sim 1.44 \times 10^{13}\,\mathrm{cm}^{-2}$ after removing the IL, which is much lower than the pristine counterparts ($2.17 \times 10^{13}\,\mathrm{cm}^{-2}$ at 2 K). The evidence of temperature-independent and suppression of n_s could suggest that oxygen vacancies annihilated during the gating process. The suppressed oxygen vacancies at the interface are due to the oxygen that electromigrated from the capping layer into STO filling the oxygen vacancies.[31] This oxygen electromigration is in accordance with previous reports, where oxygen is effectively modulated by gating.[31,41] It seems like that oxygen vacancies are filled only in the amorphous capping layer 2DEG systems (amorphous-LAO/STO or amorphous-GAO/STO) based on the previous work by electrolyte gating.[31,42] However, our 2DEG at the interface of single-crystal CZO/STO could also achieve this oxygen vacancy filling by the electromigration. Due to the low R_s and n_s as a result of the oxygen electromigration process, μ is enhanced nearly twice at low temperatures.

To further elucidate the underlying mechanisms on the MIT and the oxygen migration, a schematic illustration of the GAO/STO (or LAO/STO) and CZO/STO devices is shown in Fig. 5. After introducing the IL on the surface of the GAO/STO (or LAO/STO) device [Fig. 5(a)], cations and anions are distributed randomly at $V_g = 0$ V, thus no electrostatic gating effect occurs. Whereas in the case of CZO/STO, polarization originating from the lattice distortion under compressive strain has been theoretically predicted and experimentally proved.[14,40] The polarization pointing toward the interface could play a similar role in applying a negative electrostatic gating, as shown in Fig. 5(b). Under this circumstance, even at $V_g = 0$ V, anions accumulate above the surface of the CZO thin film, and electrons in the channel are therefore depleted. This explains why the MIT occurs while the n_s is suppressed from $4.9 \times 10^{13}\,\mathrm{cm}^{-2}$ to $5.5 \times 10^{12}\,\mathrm{cm}^{-2}$ after immersion in the IL. In Fig. 5(c), on applying a positive V_g, the electrostatic potential counteracts with this negative electrostatic-like effect. Electrons therefore get accumulated and the CZO/STO device shows the metallic behavior again. Besides the above electrostatic process, an electrochemical effect based on the movement of ions also occurs during the electrolyte gating. On applying a negative gate voltage, electrons at the interface get depleted and the oxygen electromigrated from CZO to the interface, i.e., the surface of STO, as schematically illustrated in Fig. 5(d), thus resulting in the filling of oxygen vacancies. The n_s is therefore suppressed and shows a temperature-independent behavior. Time-dependent sheet resistance with different V_g at room temperature, as shown in Fig. S6, further indicates that the oxygen electromigration process occurs only during the negative bias process. On applying a positive V_g, the sheet resistance decreases and then

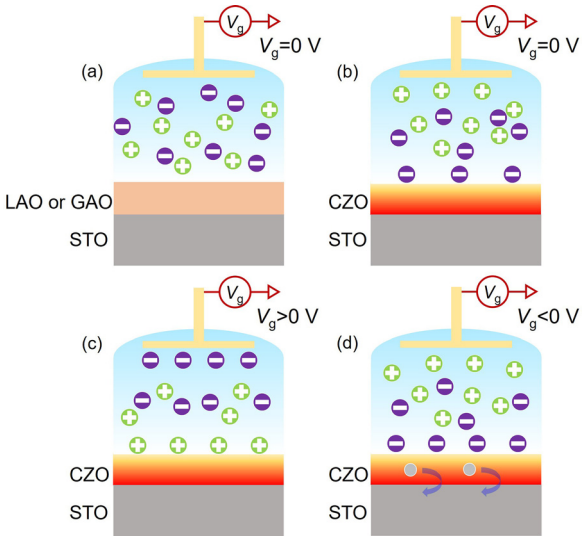

FIG. 5. The schematic diagrams for the distribution of ions in the IL for the oxide 2DEG EDLT. (a) Anions and cations are distributed randomly at $V_g = 0$ V for the LAO/STO or GAO/STO heterointerfaces. (b) Anions are accumulated above the CZO surface with no gate voltage applied for the CZO/STO. This situation is similar to the one applied with a negative bias. (c) By applying a positive V_g, cations move close to the CZO/STO heterointerface, an electronic double layer is formed, and more electrons are accumulated at the interface. (d) The oxygen electromigration from CZO to STO via applying a negative bias. Oxygen vacancies are filled.

recovers to its original state when setting $V_g = 0$ V, which is a typical and reversible electrostatic effect, and no oxygen vacancies are filled. In contrast, on applying a negative bias, the sheet resistance increases sharply and cannot recover to its original state after the negative bias. This irreversible behavior indicates that the oxygen vacancies are filled only after the application of negative V_g.

As previously demonstrated, the devices are easily degraded during the IL gating period, which is the primary limit for the electrolyte gating application. For example, 2D materials, $La_{0.5}Sr_{0.5}CoO_{3-x}$ and STO, are likely damaged due to the electrochemical reactions without special care.[43–45] In order to prevent being damaged by IL gating, boron nitride or graphene buffer is inserted between the IL and materials.[46,47] Similar to the role of these buffer layers, the capping layer of CZO could prevent the IL gating induced damage for the interfacial 2DEG. This is further proved by the surface characterization by AFM, as shown in Fig. S7. The surfaces before and after gating remain significantly similar. Moreover, the leakage current (<1 nA) is much smaller than the applied current (1 μA) for transport measurements, as shown in Fig. S5. This negligible leakage current indicates that oxygen electromigration occurs only at the interface of CZO/STO, rather than the CZO surface in contact with the IL.

In conclusion, we have demonstrated the electrolyte gating on the 2DEG originating from the strain induced polarization at the isostructural perovskite-type interface of CZO/STO. Besides the conventional effective tuning of R_s, n_s, and μ, as realized via IL gating with the EDLT configuration, an astonishing MIT occurs upon exposure of the sample surface to the IL even without the gate voltage. This could be a direct evidence of the presence of polarization of the CZO capping layer. Furthermore, oxygen electromigration induced by IL gating otherwise suppresses the oxygen vacancies and significantly improves the

quality of the 2DEG at the CZO/STO interface. Our finding reveals an intrinsic difference between the nonpolar oxide interfaces with the intensively investigated polar oxide interfaces.

See the supplementary material for details on complete surface characterization, basic mechanism of IL gating, comparisons with the samples of LAO/STO and GAO/STO, leakage current, and the sheet resistance as a function of time under V_g of the CZO/STO heterointerface.

This work was supported by the National Key Research and Development Program of China (Grant No. 2017YFA0206304), the National Natural Science Foundation of China (Grant Nos. 11874203, 61822403, 61874060, and U1732159), Jiangsu Specially Appointed Professor program, Natural Science Foundation of Jiangsu Province (Grant No. BK20181388), Oversea Researcher Innovation Program of Nanjing, NUPTSF (Grant No. NY217118), and the Fundamental Research Funds for the Central Universities (Grant No. 021014380080). W. Q. Liu acknowledges the financial support from UK EPSRC EP/S010246/1, Royal Society IEC\NSFC\181680, and Leverhulme Trust LTSRF1819\15\12. Niu thanks Dr. Hongrui Zhang for useful discussions.

REFERENCES

[1]A. Ohtomo and H. Y. Hwang, Nature **427**(29), 423 (2004).
[2]N. Reyren, S. Thiel, A. D. Caviglia, L. F. Kourkoutis, G. Hammerl, C. Richter, C. W. Schneider, T. Kopp, A.-S. Rüetschi, D. Jaccard, M. Gabay, D. A. Muller, J.-M. Triscone, and J. Mannhart, Science **317**, 1196 (2007).
[3]J. A. Bert, B. Kalisky, C. Bell, M. Kim, Y. Hikita, H. Y. Hwang, and K. A. Moler, Nat. Phys. **7**(10), 767 (2011).
[4]D. V. Christensen, Y. Frenkel, Y. Z. Chen, Y. W. Xie, Z. Y. Chen, Y. Hikita, A. Smith, L. Klein, H. Y. Hwang, N. Pryds, and B. Kalisky, Nat. Phys. **15**, 269 (2019).
[5]F. Trier, G. E. Prawiroatmodjo, Z. Zhong, D. V. Christensen, M. von Soosten, A. Bhowmik, J. M. Lastra, Y. Chen, T. S. Jespersen, and N. Pryds, Phys. Rev. Lett. **117**(9), 096804 (2016).
[6]G. Cheng, M. Tomczyk, A. B. Tacla, H. Lee, S. Lu, J. P. Veazey, M. Huang, P. Irvin, S. Ryu, C.-B. Eom, A. Daley, D. Pekker, and J. Levy, Phys. Rev. X **6**(4), 041042 (2016).
[7]Y. Lei, Y. Li, Y. Z. Chen, Y. W. Xie, Y. S. Chen, S. H. Wang, J. Wang, B. G. Shen, N. Pryds, H. Y. Hwang, and J. R. Sun, Nat. Commun. **5**, 5554 (2014).
[8]S. Thiel, G. Hammerl, A. Schmehl, C. W. Schneider, and J. Mannhart, Science **313**, 1942 (2006).
[9]Y. Chen, N. Pryds, J. E. Kleibeuker, G. Koster, J. Sun, E. Stamate, B. Shen, G. Rijnders, and S. Linderoth, Nano Lett. **11**(9), 3774 (2011).
[10]Y. Z. Chen, N. Bovet, F. Trier, D. V. Christensen, F. M. Qu, N. H. Andersen, T. Kasama, W. Zhang, R. Giraud, J. Dufouleur, T. S. Jespersen, J. R. Sun, A. Smith, J. Nygard, L. Lu, B. Buchner, B. G. Shen, S. Linderoth, and N. Pryds, Nat. Commun. **4**, 1371 (2013).
[11]W. Niu, Y. Gan, Y. Zhang, D. V. Christensen, M. von Soosten, X. Wang, Y. Xu, R. Zhang, N. Pryds, and Y. Chen, Appl. Phys. Lett. **111**, 021602 (2017).
[12]M. Zhang, Z. Chen, B. Mao, Q. Li, H. Bo, T. Ren, P. He, Z. Liu, and Y. Xie, Phys. Rev. Mater. **2**(6), 065002 (2018).
[13]Y.-Y. Pai, A. Tylan-Tyler, P. Irvin, and J. Levy, Rep. Prog. Phys. **81**(3), 036503 (2018).
[14]Y. Chen, F. Trier, T. Kasama, D. V. Christensen, N. Bovet, Z. I. Balogh, H. Li, K. T. S. Thydén, W. Zhang, S. Yazdi, P. Norby, N. Pryds, and S. Linderoth, Nano Lett. **15**(3), 1849 (2015).
[15]J. P. Ibbetson, P. T. Fini, K. D. Ness, S. P. DenBaars, J. S. Speck, and U. K. Mishra, Appl. Phys. Lett. **77**(2), 250 (2000).
[16]A. Tsukazaki, A. Ohtomo, T. Kita, Y. Ohno, H. Ohno, and M. Kawasaki, Science **315**(9), 1388 (2007).
[17]J. Cheng, S. Nazir, and K. Yang, ACS Appl. Mater. Interfaces **8**(46), 31959 (2016).
[18]L. Chen, J. Li, Y. Tang, Y. Y. Pai, Y. Chen, N. Pryds, P. Irvin, and J. Levy, Adv. Mater. **30**, 1801794 (2018).
[19]C. Leighton, Nat. Mater. **18**(1), 13 (2019).
[20]S. Z. Bisri, S. Shimizu, M. Nakano, and Y. Iwasa, Adv. Mater. **29**, 1607054 (2017).
[21]W.-N. Lin, J.-F. Ding, S.-X. Wu, Y.-F. Li, J. Lourembam, S. Shannigrahi, S.-J. Wang, and T. Wu, Adv. Mater. Interfaces **1**(1), 1300001 (2014).
[22]S. Zeng, W. Lu, Z. Huang, Z. Liu, K. Han, K. Gopinadhan, C. Li, R. Guo, W. Zhou, H. H. Ma, L. Jian, T. Venkatesan, and Ariando, ACS Nano **10**(4), 4532 (2016).
[23]W. Niu, Y. Zhang, Y. Gan, D. V. Christensen, M. V. Soosten, E. J. Garcia-Suarez, A. Riisager, X. Wang, Y. Xu, R. Zhang, N. Pryds, and Y. Chen, Nano Lett. **17**(11), 6878 (2017).
[24]J. T. Yang, C. Ge, J. Y. Du, H. Y. Huang, M. He, C. Wang, H. B. Lu, G. Z. Yang, and K. J. Jin, Adv. Mater. **30**, 1801548 (2018).
[25]N. Lu, P. Zhang, Q. Zhang, R. Qiao, Q. He, H. B. Li, Y. Wang, J. Guo, D. Zhang, Z. Duan, Z. Li, M. Wang, S. Yang, M. Yan, E. Arenholz, S. Zhou, W. Yang, L. Gu, C. W. Nan, J. Wu, Y. Tokura, and P. Yu, Nature **546**(7656), 124 (2017).
[26]J. Jeong, N. Aetukuri, T. Graf, T. D. Schladt, M. G. Samant, and S. S. P. Parkin, Science **339**(22), 1402 (2013).
[27]T. D. Schladt, T. Graf, N. B. Aetukuri, M. Li, A. Fantini, X. Jiang, M. G. Samant, and S. S. P. Parkin, ACS Nano **7**(9), 8074 (2013).
[28]M. Li, W. Han, X. Jiang, J. Jeong, M. G. Samant, and S. S. Parkin, Nano Lett **13**(10), 4675 (2013).
[29]C. Ge, K.-J. Jin, L. Gu, L.-C. Peng, Y.-S. Hu, H.-Z. Guo, H.-F. Shi, J.-K. Li, J.-O. Wang, X.-X. Guo, C. Wang, M. He, H.-B. Lu, and G.-Z. Yang, Adv. Mater. Interfaces **2**(17), 15004407 (2015).
[30]L. Zhang, S. Zeng, X. Yin, T. C. Asmara, P. Yang, K. Han, Y. Cao, W. Zhou, D. Wan, C. S. Tang, A. Rusydi, Ariando, and T. Venkatesan, ACS Nano **11**, 9950 (2017).
[31]S. W. Zeng, X. M. Yin, T. S. Herng, K. Han, Z. Huang, L. C. Zhang, C. J. Li, W. X. Zhou, D. Y. Wan, P. Yang, J. Ding, A. T. S. Wee, J. M. D. Coey, T. Venkatesan, A. Rusydi, and A. Ariando, Phys. Rev. Lett. **121**, 146802 (2018).
[32]K. H. Lee, M. S. Kang, S. Zhang, Y. Gu, T. P. Lodge, and C. D. Frisbie, Adv. Mater. **24**(32), 4457 (2012).
[33]S. Wu, X. Luo, S. Turner, H. Peng, W. Lin, J. Ding, A. David, B. Wang, G. Van Tendeloo, J. Wang, and T. Wu, Phys. Rev. X **3**(4), 041027 (2013).
[34]S. Das, Z. Hossain, and R. C. Budhani, Phys. Rev. B **94**(11), 115165 (2016).
[35]E. Maniv, M. B. Shalom, A. Ron, M. Mograbi, A. Palevski, M. Goldstein, and Y. Dagan, Nat. Commun. **6**, 8239 (2015).
[36]Y. Zhang, Y. Gan, W. Niu, K. Norrman, X. Yan, D. V. Christensen, M. V. Soosten, H. Zhang, B. Shen, N. Pryds, J. Sun, and Y. Chen, ACS Appl. Mater. Interfaces **10**(1), 1434 (2018).
[37]Y. L. Gan, D. V. Christensen, Y. Zhang, H. R. Zhang, D. Krishnan, Z. Zhong, W. Niu, D. J. Carrad, K. Norrman, M. von Soosten, T. S. Jespersen, B. G. Shen, N. Gauquelin, J. Verbeeck, J. R. Sun, N. Pryds, and Y. Z. Chen, Adv. Mater. **31**, 1805970 (2019).
[38]Y. Zhou, P. Wang, Z. Z. Luan, Y. J. Shi, S. W. Jiang, H. F. Ding, and D. Wu, Appl. Phys. Lett. **110**(14), 141603 (2017).
[39]Y. Xie, Y. Hikita, C. Bell, and H. Y. Hwang, Nat. Commun. **2**, 494 (2011).
[40]S. Nazir, J. Cheng, and K. Yang, ACS Appl. Mater. Interfaces **8**(1), 390 (2016).
[41]C. W. Bark, P. Sharma, Y. Wang, S. H. Baek, S. Lee, S. Ryu, C. M. Folkman, T. R. Paudel, A. Kumar, S. V. Kalinin, A. Sokolov, E. Y. Tsymbal, M. S. Rzchowski, A. Gruverman, and C. B. Eom, Nano Lett. **12**(4), 1765 (2012).
[42]D. V. Christensen, F. Trier, Y. Z. Chen, A. Smith, J. Nygård, and N. Pryds, Appl. Phys. Lett. **102**(2), 021602 (2013).
[43]J. T. Ye, Y. J. Zhang, Y. Kasahara, and Y. Iwasa, Eur. Phys. J. **222**(5), 1185 (2013).
[44]J. Walter, H. Wang, B. Luo, C. D. Frisbie, and C. Leighton, ACS Nano **10**(8), 7799 (2016).
[45]K. Ueno, H. Shimotani, Y. Iwasa, and M. Kawasaki, Appl. Phys. Lett. **96**(25), 252107 (2010).
[46]Y. Zhou, J. Park, J. Shi, M. Chhowalla, H. Park, D. A. Weitz, and S. Ramanathan, Nano Lett. **15**(3), 1627 (2015).
[47]P. Gallagher, M. Lee, T. A. Petach, S. W. Stanwyck, J. R. Williams, K. Watanabe, T. Taniguchi, and D. Goldhaber-Gordon, Nat. Commun. **6**, 6437 (2015).